SCIENCE CHINA
Technological Sciences

Special Topic: Mechanical Engineering
• Article •

November 2016 Vol.59 No.11: 1656–1665
doi: 10.1007/s11431-016-0206-6

New forming method of manufacturing cylindrical parts with nano/ultrafine grained structures by power spinning based on small plastic strains

XIAO GangFeng[1], XIA QinXiang[1*], CHENG XiuQuan[2] & LONG Hui[3]

[1] *School of Mechanical and Automotive Engineering, South China University of Technology, Guangzhou 510640, China;*
[2] *Department of Aircraft Maintenance Engineering, Guangzhou Civil Aviation College, Guangzhou 510403, China;*
[3] *Department of Mechanical Engineering, The University of Sheffield, Sheffield S1 3JD, UK*

Received March 16, 2016; accepted June 19, 2016; published online October 11, 2016

A new spinning method to manufacture the cylindrical parts with nano/ultrafine grained structures is proposed, which consists of quenching, power spinning and recrystallization annealing. The microstructural evolution during the different process stages and macroforming quality of the spun parts made of ASTM 1020 steel are investigated. The results show that the microstructures of the ferrites and pearlites in the ASTM 1020 steel are transformed to the lath martensites after quenching. The martensite laths obtained by quenching are refined to 87 nm and a small amount of nanoscale deformation twins with an average thickness of 20 nm is generated after performing a 3-pass stagger spinning with 55% thinning ratio of wall thickness, where the equivalent strain required is only 0.92. The equiaxial ferritic grains with an average size of 160 nm and nano-carbides are generated by subsequent recrystallization annealing at 480°C for 30 min. The spun parts with high dimensional precision and low surface roughness are obtained by the forming method developed in this work, combining quenching with 3-pass stagger spinning and recrystallization annealing.

nano/ultrafine grained structure, cylindrical parts, quenching, power spinning, recrystallization annealing, small plastic strain

Citation: Xiao G F, Xia Q X, Cheng X Q, et al. New forming method of manufacturing cylindrical parts with nano/ultrafine grained structures by power spinning based on small plastic strains. Sci China Tech Sci, 2016, 59: 1656–1665, doi: 10.1007/s11431-016-0206-6

1 Introduction

The nano and ultrafine grained structures refer to the materials whose grain size is ranged from 1 to 100 nm and from 100 to 1000 nm, respectively [1]. It has attracted significant interests in scientific research and industry application due to its unique mechanical, physical and chemical properties [2]. Plastic deformation is one of the important methods to refine the grain structure of metal materials to nano or ultrafine scale. In order to manufacture materials with nano/ultrafine structures, severe plastic deformation (SPD) methods, such as equal channel angular pressing (ECAP) [3], high pressure torsion (HPT) [4], multiple forging (MF) [5], accumulative roll bonding (ARB) [6], etc. have been proposed and reported. The SPD processes are characterized by inducing the plastic deformation on the same region of material repeatedly. Large plastic strains and complicated material process procedures are required in the reported SPD processes [7]. However for carbon steel materials, the minimum strain necessary for manufacturing nanocrystalline structures is considered to be around 7~8, as reported by Umemoto [8]. Therefore, the production of ultrafine

*Corresponding author (email: meqxxia@scut.edu.cn)

grained (UFG) steels by these SPD processes is limited at the laboratory scale, and the application of the SPD methods in industrial applications is extremely difficult [9].

Metal spinning belongs to a near net-shape forming technology. During spinning, a continuous and localized plastic deformation occurs in the metal blank to form an axis-symmetrical hollow part by means of roller feeding movement and rotational motion of the mandrel [10–12]. Flow forming, as a power spinning process, can be used to manufacture cylindrical parts with nano/ultrafine grained structures [13]. Xia et al. [14] has developed a forming procedure to produce the cylindrical parts with nano/ultrafine grain structures by stagger spinning and recrystallization annealing (SA). By using the developed process procedure, the ferritic grains with an average initial size of 50 μm are refined to 600 nm with the equivalent strain of 2.27 (the corresponding thinning ratio of wall thickness is 87%), which is much smaller than that of the above reported SPD. However the thinning ratio of wall thickness will exceed 90% if the grain sizes are further refined by the SA method, which would cause difficulties in controlling the macroforming quality of the spun part because of the high thinning ratios induced.

To obtain bulk metal components with nano/ultrafine grained structures for industry applications, the material deformation required for refining coarse grains to nano or ultrafine scale should be reduced to lower levels, which is not only necessary in reducing the forming processes required, but also in controlling the macroforming quality.

In the present work, a new forming method to manufacture cylindrical parts with nano/ultrafine grained structures by power spinning with small plastic strains has been proposed and experimentally tested. An average grain size of 160 nm is obtained under the equivalent strain of only 0.92 based on the proposed forming method. The macroforming quality of the cylindrical part and the microstructural evolution during the proposed material process procedure are investigated in details.

2 Development of forming method for nano/ultrafine grained structures

2.1 Overall process design

The grain size of materials is closely related to the microstructure of the original material, the degree of deformation and heat treatment conditions after plastic deformation [15]. Ueji et al. [16] suggested that the fine grained structure of martensite played an important role in subdivision of microstructures for achieving the ultrafine grain during plastic deformation. For low carbon steels, the lath martensite obtained by quenching has a hierarchical multi-scale of microstructures, including packets, blocks and laths, where the packets and blocks have high-angle boundaries, which refine the prior austenite grains greatly during martensite transformation [17]. Yang et al. [18] pointed out that the lath martensite has the finest structure among all microstructures of low carbon steels, thus the required plastic strain may be reduced if the lath martensite is used as the initial microstructure to manufacture the parts with nano/ultrafine grained structures. Quenching is the best method for refining the microstructure which introducing a large number of dislocations through heat treatment.

Grains stretch along the deformation direction resulting in fibrous tissue to be formed after plastic deformation. Xia et al. [14] achieved the results of transforming the severe deformed grains with high density of dislocation to equiaxed ultrafine grains without distortion by means of recrystallization. Therefore, the method based on quenching, power spinning and recrystallization annealing is proposed in this study to manufacture the cylindrical parts with nano/ultrafine grained structures.

The forming method developed consists of the following stages: firstly, the cylindrical blanks are austenitized and then cooled quickly in the quenching medium to form the martensite. Then the 3-pass power spinning process is performed, which not only to obtain the final required shape of the parts but also to further refine the microstructure and improve the density of dislocation. Finally, the spun part with martensitic structure is subsequently annealed to form the equiaxed grains.

2.2 Determination of process parameters for quenching

For the hypo-eutectoid steel, to obtain the fine martensitic structure, the quenching temperature (T_q) is 30°C–50°C above Ac_3, where Ac_3 is the transformation temperature from ferrite and cementite to austenitic during heating. The temperature of Ac_3 for ASTM 1020 is about 860°C, therefore, the range of the quenching temperature T_q of ASTM 1020 is 890°C–910°C. To improve the hardenability, the temperature should be as high as possible. Therefore, T_q is selected as 910°C in this study to obtain the fine and homogenous austenitic grains. The samples are put into the heat resistance furnace when the temperature is increased to T_q (point *A*), as shown in Figure 1.

The austenizating holding time, τ_1, can be calculated theoretically by using eq. (1) [19]

$$\tau_1=Kt, \tag{1}$$

where K is a coefficient valued as 2.5 min/mm; t is the thickness of the parts. The wall thickness of the cylindrical blank is 4 mm, therefore, the holding time is 10 min.

To obtain the martensitic structure, the cooling rate should be quick during quenching. The commonly used quenching media include water, oil and 5% NaCl solution. The cooling rate using the water or oil as quenching media is slow at the high temperature zone; while the cooling rate

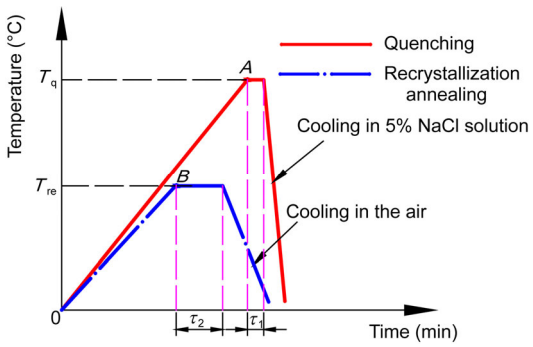

Figure 1 (Color online) Schematic diagram of the heat treatment.

using the 5% NaCl solution as the quenching medium improves considerably at the high temperature zone. This is due to the fact that the hot surface of the quenching workpiece is covered by the NaCl solution, and the steam film of water will be ruptured by the precipitation and violent explosion of the NaCl crystals. Therefore, the 5% NaCl solution is selected as the quenching media in this study.

2.3 Determination of power spinning process

Flow forming, classified as a power spinning process, is an important method to manufacture hollow cylindrical parts with thin-walled thickness. It mainly consists of two groups of processes, stagger spinning and counter-roller spinning, as outlined by Zeng et al. [20]. Stagger spinning is a traditional power spinning process. Typically, two or more rollers (usually three rollers) are used during processing, and there is a certain distance between rollers along both the axial and radial directions, as shown in Figure 2 [14]. Counter-roller spinning is a novel mandrelless power spinning process. Typically, one or more pairs of rollers are used during processing, and the mandrel is replaced by the inner rollers thus the mandrel is no longer required [21]. During the counter-roller spinning, the inner and outer surfaces of the cylindrical blanks deformed simultaneously, the distribution of equivalent strains and grain refinement of spun parts obtained by the counter-roller spinning are more homogeneous, compared to the stagger spinning [21]. However, the martensite is a type of non-equilibrium structures with high internal stresses, and these internal stresses will be further increased after power spinning, the distortion will be induced at the deformed area of the workpiece, especially at the opening area of the workpiece, as shown in Figure 3. During counter-roller spinning, severe distortion occurs at the opening area of the workpiece after one pass spinning due to no mandrel support, which becomes an obstacle of the subsequent spinning process. Therefore, the counter-roller spinning is not suitable for forming of parts with the martensitic structure.

For manufacturing of cylindrical parts, backward power spinning is commonly used. During backward spinning, the

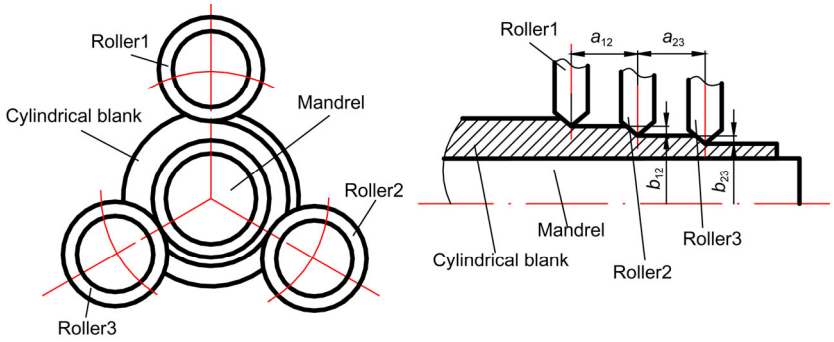

Figure 2 (Corlor online) Illustration of stagger power spinning.

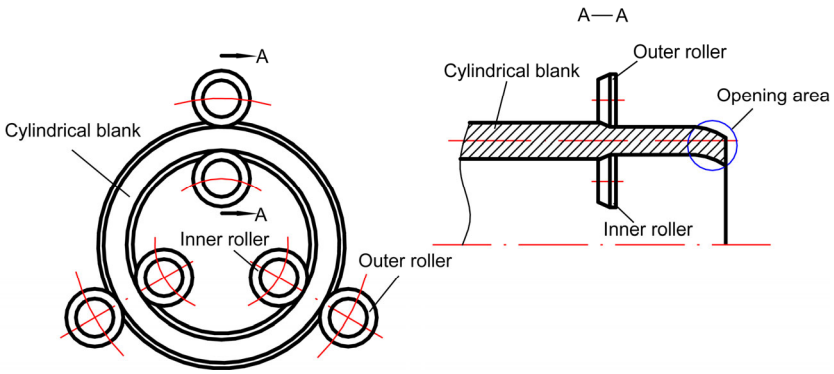

Figure 3 (Color online) Distortion of the spun parts during the counter-roller spinning.

deformed material at the contact zones is in a state of three-dimensional compressive stress, which improves the formability of the material and beneficial to the refinement of grains, as reported by Xia et al. [14]. Therefore, the three roller backward stagger spinning is adopted in this study.

2.4 Determination of process parameters for recrystallization annealing

The recrystallization temperature, T_{re}, can be calculated theoreticallly by using eq. (2) [22]

$$T_{re}=\delta T_m, \tag{2}$$

where δ is a coefficient valued as 0.35–0.4; T_m is the melting temperature of the material.

The melting temperature of the ASTM 1020 is about 1600°C, therefore, the T_{re} of the ASTM is about 525°C–600°C. As reported, the T_{re} of the spun parts under 87% thinning ratio is 580°C [14]. The density of the dislocation and stored energy obtained by quenching and power spinning is much larger than that of obtained by the power spinning, therefore, the recrystallization temperature of the deformed martensite parts should be lower than 580°C. In this study the temperature range of the recrystallization annealing is selected from 430°C to 580°C. The samples are put into the heat resistance furnace when the temperature is increased to T_{re} (point *B*), as shown in Figure 1.

The holding time of the recrystallization annealing is selected as 60 min for the ASTM 1020 spun parts under 87% thinning ratio of wall thickness, as reported by Xia et al. [14]. However, for the spun parts with martensite, the deformed martensitic structure will be decomposed into double phase structures of the ferrite and cementite during the subsequent annealing process. The fine and homogeneous cementite particles which act as precipitated phase in the microstructure are necessary to prevent the growth of the ferrite grains during the annealing. Therefore, to prevent the carbon agglomeration and growth, the holding time should be shorter than that of the conventional recrystallization annealing. The time of the martensite decomposing into ferrite and the cementite, τ_2, can be calculated theoreticallly by using eq. (3) [19]

$$\tau_2=K+At, \tag{3}$$

where K is time-base, for box-type resistance furnace, the value is 20 min; A is a coefficient, the value is 2.5 min/mm; t is the thickness of the workpiece. Therefore, the holding time is calculated as 30 min, as shown in Figure 1.

3 Experimental tests

3.1 Test conditions of power spinning

The power spinning experiment is carried out on the HGPX-WSM CNC spinning machine (Figure 4) [23], the stagger spinning device adopted in the experiment is shown in Figure 5 [14].

The tubular blanks used for the experiment are the annealed seamless ASTM 1020 steel tubes, the dimensions are 68 mm×4 mm×70 mm, and the microstructure is the ferritic and pearlite grains with an average size of 50 μm, as shown in Figure 6.

In flow forming, the double-tapered roller is usually used for forming the cylindrical blank with the medium thickness, usually in the range of 2–8 mm [24]. The key geometric dimensions of rollers are determined as follows [14]: forming angle α_ρ=25°, sleeking angle β=3°, receding angle β'=30°, roundness radius r_ρ=6 mm and polishing belt length l=1.3 mm, as shown in Figure 7.

3.2 Process parameters of power spinning

The macroforming quality and microstructure of spun part

Figure 4 (Color online) HGPX-WSM type CNC spinning machine [23].

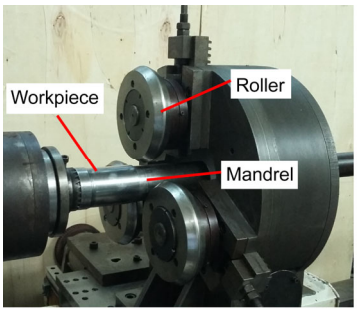

Figure 5 (Coor online) Stagger spinning devices [14].

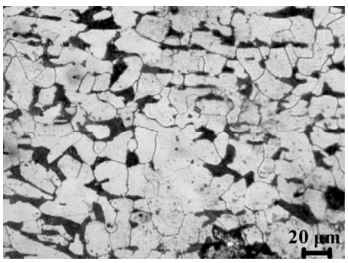

Figure 6 Initial microstructure of ASTM 1020.

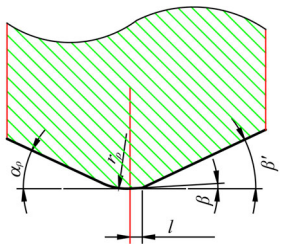

Figure 7 (Color online) Key geometric dimensions of rollers [14].

are directly influenced by the spinning process parameters. For stagger spinning, main process parameters influencing the macroforming quality and microstructure of spun parts are the feed rate of roller f, the thinning ratio per pass ψ_i ($\psi_i=(t_{i-1}-t_i)/t_{i-1}$, where t_{i-1} is the wall thickness of the cylindrical parts after $i-1$ passes spinning, t_i is the wall thickness of the cylindrical parts after i passes spinning), and the axial offset a and radial offset b [14].

For flow forming, the optimum thinning ratio per pass ψ_i for cylindrical blank power spinning is 30%–45%, as reported by Xia et al. [14]. According to Wang and Liu [25], for low-carbon steel, the feed rate of roller should be in the range of 0.2–1.0 mm/r. Considering both process efficiency and forming quality, the feed rate of roller f is selected as 0.6 mm/r in this study [26]. The value of the axial offset a and radial offset b (as illustrated in Figure 2) during stagger spinning should be marched to keep the radial force undertaken by each roller being equilibrated, where the calculated values of the axial offset a_{12} and a_{23} are very close. The value of axial offset should be rounded to be easily implemented in the experiment, so the values of the axial offset a_{12} and a_{23} can be selected as the same, as listed in Table 1 [14]. The rotational speed of mandrel n has not shown obvious influence on the macroforming quality, as reported by Xia et al. [27]. Therefore, the rotational speed n is selected as 108 r/min based on the capacity of the spinning machine [14].

3.3 Analysis methods of microstructure

To study the microstructural evolution in manufacturing the cylindrical parts with nano/ultrafine grained structures, microstructural observations are carried out during all stages of the process procedures.

To observe the grain morphology of the workpiece, the optical microscopy (OM) observation is carried out by the LEICA DMI 5000M intelligent metallographic microscope. The samples are etched by the 4% HNO_3+96% $C_2H_4O_2$ solution, which are cut from the stable spinning area of the spun workpiece. The cutting distance from the opening area of the spun workpiece is about 15 mm, and the microstructures of the samples along the longitudinal section are observed, as shown in Figure 8.

To observe the dislocation density and grain size of the workpiece with the nano/ultrafine structures, the TEM observation is carried out by using a JEM-2100 instrument. The TEM samples are prepared by the mechanical polishing to the thickness of 50 μm, followed by twin-jet electropolishing in 4% $HClO_4$+96% $C_2H_4O_2$ solution at –40°C and 75 V voltages. The corresponding selected area electron diffraction (SAED) patterns are taken with an aperture size of 700 nm. The cutting position of the samples for TEM observation is the same as that of the OM observation, and the microstructures on the surfaces of the samples are observed, as shown in Figure 8.

4 Results and discussion

4.1 Microstructural evolution

To reduce the required plastic strain in manufacturing cylindrical parts with nano/ultrafine grained structures, martensite with high density dislocation and refined microstructure is used as the initial microstructure for power spinning. Figure 9 shows the optical micrograph of the cylindrical blank after austenitized at 910 C for 10 min and cooled in 5% NaCl solution. It shows that the microstructure of the ASTM 1020 are transformed from the ferrite and pearlite to the lath martensite, but the average grain size of austenite increases from 50 to 100 μm due to the grain coarsening during austenitization.

For carbon steels, the martensite start temperature, Ms, can be calculated by using eq. (4) [28]

$$M\text{s}=520-(\text{C}\%)\times 320, \tag{4}$$

where C% is the carbon content of the material.

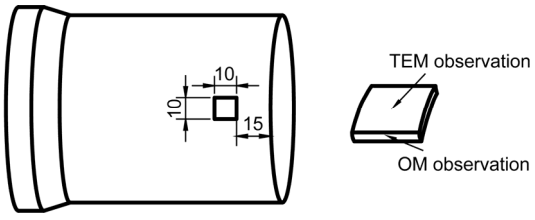

Figure 8 Samples cut for the OM and TEM observation.

Table 1 Process parameters of stagger spinning

Pass	Thinning ratio ψ_i (%)	Axial offset axial offset a (mm)	Radial offset b_{12} (mm)	Radial offset b_{23} (mm)
1	35	2.5	0.45	0.35
2	33	2.5	0.25	0.25
3	31	2.5	0.20	0.20

Figure 9 Optical micrograph of the cylindrical blank after austenitized at 910°C for 10 min and cooled in 5% NaCl solution.

The martensite start temperature of the ATSM 1020 steel is 456°C according to eq. (4). The amount of the martensite transformation is determined by the cooling temperature and can be calculated by using eq. (5) [22]

$$\varphi=1-\exp(-1.10\times10^{-2}\Delta T), \quad (5)$$

where φ is volume fraction of martensite, ΔT is subcooled temperature below Ms.

After quenching, the volume fraction of lath martensite is 99% according to eq. (5). Three-level hierarchy exists in the lath martensite structure: martensite lath, block and packet, as reported by Kitahara et al. [29]. The martensite lath is a single crystal of martensite with a high density of dislocation, the block is the aggregations of the laths with the same crystallographic orientation, and the packet is the aggregations of the blocks with the same $\{111\}_\gamma$ plane in austenite, as shown in Figure 10.

Power spinning is not only the main forming procedure to obtain the final required shape of the parts, but also can further improve the dislocation density and refine the grains. Figure 11 shows the optical micrograph of the spun part after stagger spinning under 55% thinning ratio of wall thickness, where the actual thinning ratio of the spun parts is smaller than that of the designed one (listed in Table 1) due to the spring back of the spun parts. The darkly etched line is the prior austenite grain boundaries (GBs). It shows that the martensitic grains of the original isometric crystals are stretched along the deformation direction. The average hardness of the deformed martensite increases to 520 HV,

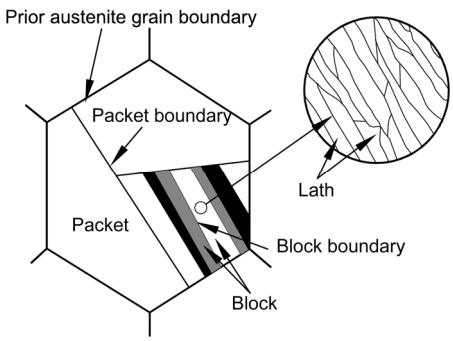

Figure 10 Microstructural hierarchy of the lath martensite [29].

which is larger than the average hardness of the martensite before spinning (440 HV). It indicates that the martensitic structure is hardened considerably after power spinning.

Figure 12 shows the TEM micrographs of the spun part after stagger spinning under 55% thinning ratio of wall

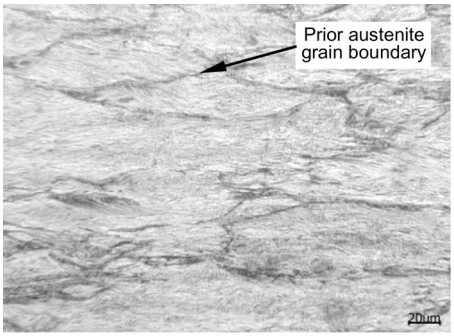

Figure 11 Optical micrograph of the spun part after stagger spinning under 55% thinning ratio.

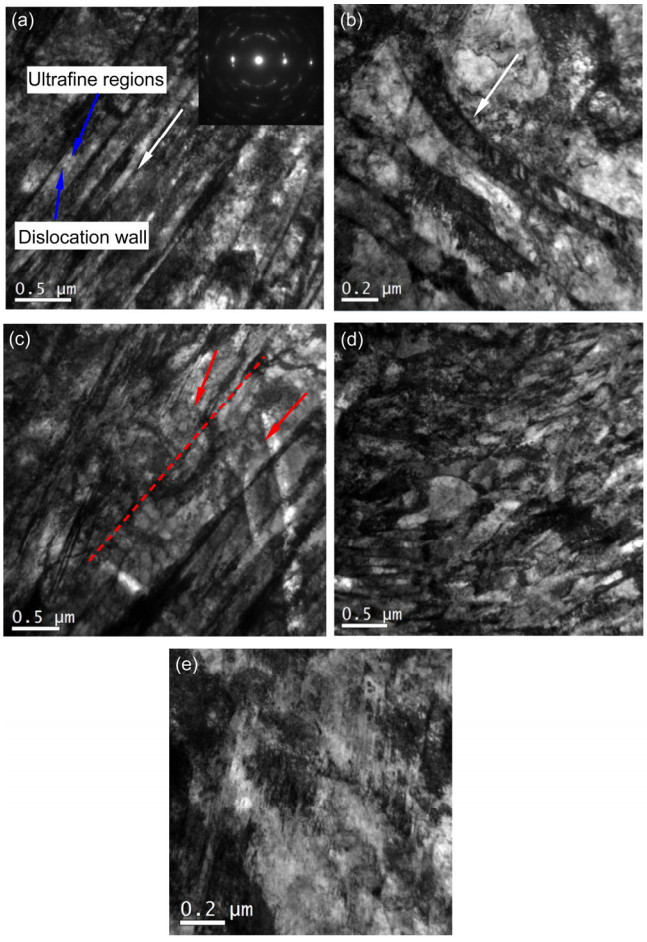

Figure 12 (Color online) TEM micrographs of spun part after stagger spinning under 55% thinning ratio. (a) Refined lamellar structure of lath martensite; (b) bent lamellar structure of lath martensite; (c) lamellar structure nearing the block boundary; (d) irregularly bent lamellar structure nearing the packet boundary; and (e) twins in the deformed martensitic structure.

thickness, the white arrow indicates the deformation direction. It shows that the microstructures with many non-equilibrium grain boundaries are distorted severely, and the distinctive contrast in the grain interiors indicates that the high level internal stresses and elastic distortions exist in the crystalline lattices. The martensite laths with high density dislocation are elongated along the direction parallel to the deformation (Figure 12(a)) and bent along the direction perpendicular to the deformation (Figure 12(b)). Inside the martensite lath, the lath is divided to ultrafine regions by the dislocation walls (Figure 12(a)). The average thickness of the martensite laths paralleling to the deformation direction is refined to 87 nm, as shown in Figure 12(a). Figure 12(a) also shows that many arc-like points are contained in the SAED pattern, which indicates that large number of high-angle boundary exists within the selected small areas.

Nevertheless, the deformation of the martensite during spinning is inhomogeneous due to the different orientations of the slip system. Figure 12(c) shows the microstructure of the martensite nearing the block boundary after spinning. The broken red line in Figure 12(c) refers to the block boundary and the red arrow refers to the orientation of the laths. It shows that the degree of refinement of the martensite laths on the left of the block boundary is much larger than that of the right. This inhomogeneous deformation may originate from the different grain orientations of the slip system. The slip system of the martensite laths on the left is located in the soft orientation. Therefore, it deforms easier and earlier than that of the martensite lath on the right, which the slip system is located in the hard orientation.

Figure 12(d) shows the microstructure of the martensite nearing the packet boundary after spinning. It shows that the irregularly bend of lamellar martensitic structure occurs due to the restriction of the packet boundaries.

In addition to the dislocation slip and pile-up, some nanoscale deformation twins also can be observed in the deformed lath martensite, as shown in Figure 12(e). It shows that the thin deformation twins with an average thickness of 20 nm are generated in the microstructure after power spinning under 55% thinning ratio of wall thickness. Dislocation slip is the dominant mechanism of the plastic deformation and twinning is rarely occurred at room temperature for the material with high stacking fault energy, such as carbon steel. However, high dislocation density and high internal stresses exist in the microstructure of the deformed martensite. The dislocation slip becomes more and more difficult during stagger spinning due to the fact that the slip resistance of the dislocation increases with the increasing of the density of dislocation. The twinning occurs inside the grains due to stress concentration at the local distorted grain boundaries (GBs) [30]. Similarly, nanoscale deformation twins are usually observed in the nanoscale copper (a material with low stacking fault energy) manufactured by SPD, as reported by Lu et al. [31].

Although the nano/ultrafine grains and sub-grains can be obtained by quenching and power spinning, the microstructure of spun part with the high density dislocation and the deformation twins is non-equilibrium. Therefore, the recrystallization annealing is necessary to obtain the equiaxed ultrafine grains without distortion.

Figure 13 shows the optical micrographs of the spun part after recrystallization annealing at 430°C–580°C for 30 min. It shows that the recrystallization is not completed when the annealing temperature is at 430°C (Figure 13(a)). The

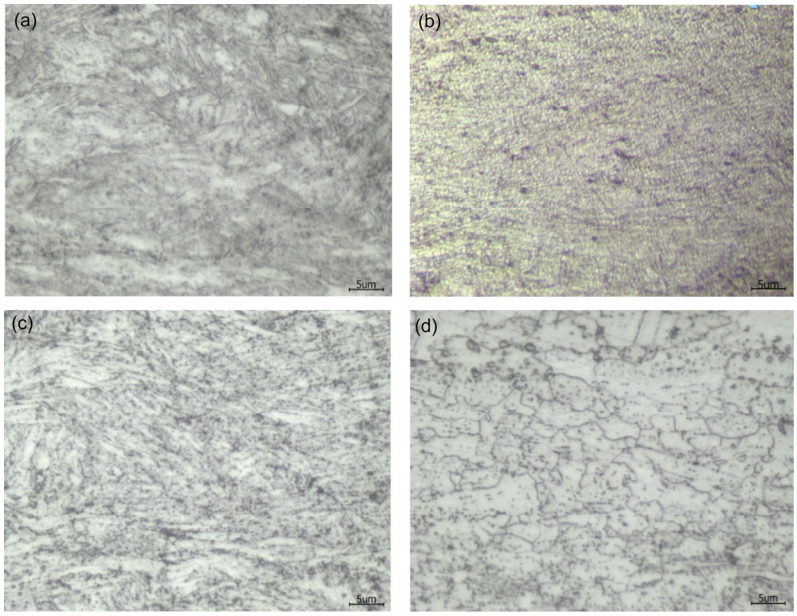

Figure 13 (Color online) Optical micrographs of the spun part after recrystallization annealing at various temperatures for 30 min. (a) 430°C; (b) 480°C; (c) 530°C; (d) 580°C.

stretched martensitic grains formed during the spinning are disappeared and the homogeneous refinement grains are generated when the annealing temperature increases to 480°C (Figure 13(b)). The grains size increases rapidly after the annealing temperature increases to 530°C–580°C (Figure 13(c) and (d)).

Figure 14 shows TEM micrograph of the spun parts under 55% thinning ratio of wall thickness after recrystallization annealing at 480°C for 30 min. It shows that the martensite laths are disappeared, the equiaxed ultrafine ferrite grains with an average grain size of 160 nm are generated and the nano-carbides are homogeneously precipitated in the GBs.

Figure 14 also shows that the SAED pattern of the spun part after recrystallization annealing contains many arc-shaped spots, which indicates that the boundaries with various misorientation angles exist at the tiny selected area. The hardness of the spun part decreases to 316.4 HV and the GBs become clearly visible, which indicates that the dislocation density of the microstructure decreases considerably and the highly internal stresses are released. Low density of dislocation inside the grains implies that the recrystallization is completed.

The equivalent strain $\bar{\varepsilon}$ ($\bar{\varepsilon}=\frac{2}{\sqrt{3}}\ln\frac{1}{1-\psi_t}$, where ψ_t is the thinning ratio of wall thickness) is only 0.92 (the thinning ratio is 55%) for the manufactured cylindrical parts with an average grain size of 160 nm in this study. The required plastic strains are much less than that by the SPD and SA methods.

The lath martensite has the hyperfine microstructures and high density dislocations, where the packets and blocks have the high-angle boundaries. The cellular substructure is generated due to the inhomogeneous distribution of the dislocation. The microstructure is further refined and many high-energy regions are generated after the power spinning. Therefore, the hyperfine microstructure with a high dislocation density and stored energy can be obtained by quenching and power spinning, the refinement degree of grains and the density of dislocation are much larger than that of the plastic deformation under the same plastic strain.

The lath martensite in the ASTM 1020 obtained by the quenching is the supersaturated solid solution of carbon, which becomes more instable after power spinning. The carbon will be precipitated in the form of cementite, and the martensite will be decomposed into the double phase structures of the ferrite and cementite after the subsequent annealing process [32]. A large number of dislocations and high stored energy as well as a small amount of twins are introduced into the microstructure after quenching and spinning, as shown in Figure 12. It provides large number of nucleation site in the high-energy regions and driving force of grain growth during the recovery and recrystallization processes [33], which contributes to the decomposition of the martensite and the nucleation of ferrite and cementite grains. On the other hand, the cementite precipitated in the GBs prevents the growth of ferrite grains, which contributes to the creation of the nano/ultrafine ferrite and cementite grains. These are the main reasons of the grain refinement leading to the nano/ultrafine scale by small plastic strain.

4.2 Macrforming quality of spun parts

The whole spinning process has been performed successfully by stagger spinning. Figure 15 shows the workpieces formed after different process stages. Yang et al. [18] experimentally verified that the thinning ratio during power spinning cannot exceed 60% to avoid the crack defects due to the low ductility of the quenched workpiece.

The relative wall thickness deviation Δ, ovality e_o, straightness e_s and roughness Ra are important indexes to evaluate the macroforming quality of spun parts, as reported by Xia et al. [26].

The wall thickness is measured at every 20 mm along axial direction and 45° along circumferential direction of the cylindrical part, as shown in Figure 16. The relative wall thickness deviation Δ is defined as the ratio of the difference between the maximum and minimum wall thickness of spun parts to the initial wall thickness of blank ($\Delta=(t_{max}-t_{min})/t_0\times100\%$, where, t_{max} is the maximum wall thickness of spun parts, t_{min} is the minimum wall thickness

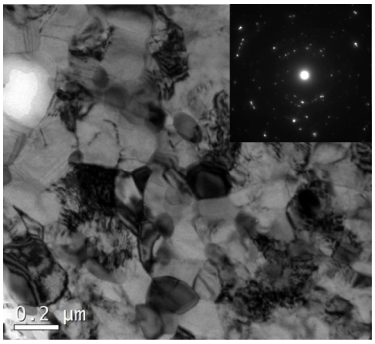

Figure 14 TEM micrograph of the spun part after recrystallization annealing at 480°C for 30 min.

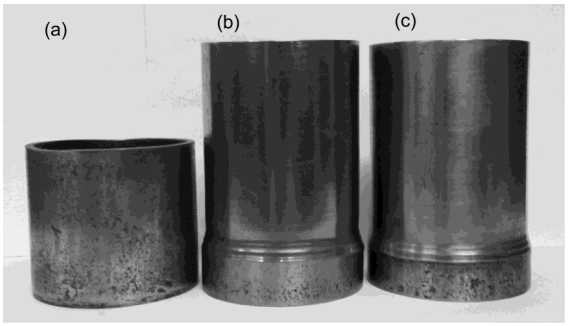

Figure 15 Workpieces formed after different process stages. (a) Quenching; (b) spinning (ψ_t=55%); (c) annealing.

of spun parts, t_0 is the initial wall thickness of blank). The ovality e_o at a certain cross section of the workpiece is defined as the difference of the maximum and minimum diameter of the workpiece at the cross section, then the ovality e_o of the workpieces means the maximum ovality at arbitrary cross section (e_o=max($D_{i\max}$–$D_{i\min}$), $D_{i\max}$ is the maximum diameter of the workpiece at the ith cross section, $D_{i\min}$ is the minimum diameter of the workpiece at the ith cross section) [34]. The straightness e_s is defined as the distance of the two nearest parallel planes, and the arbitrary generatrix on the outer surface of the workpiece is located between these two planes [34], as shown in Figure 17; where the dotted line indicates the theoretical generatrix on the outersurface of the workpiece, *A*, *C*, *E*, *G* are the measurement positions of the straightness (Figure 16(b)), d_{ga} is the distance between the point of generatrix on the outersurface of workpiece and the axis of workpiece.

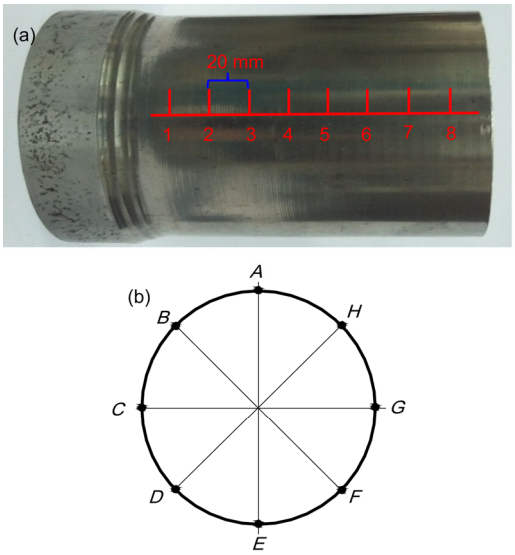

Figure 16 (Color online) Distribution of the measurement points of the wall thickness. (a) Axial direction; (b) circumferential direction.

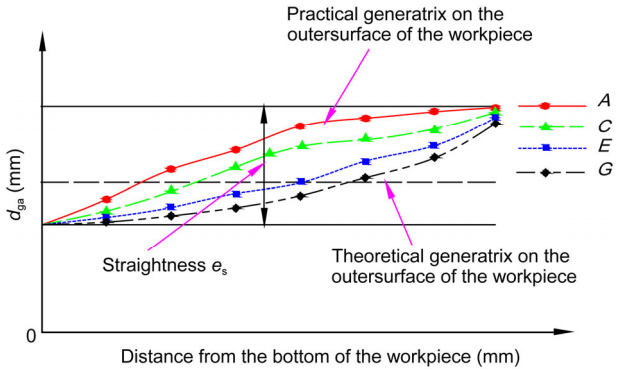

Figure 17 (Color online) Measurement of the straightness of spun workpiece.

Table 2 shows the calculated indexes of the macroforming quality under different process stages. It shows that the relative wall thickness deviation Δ of the workpiece decreases after stagger spinning. The changes of ovality e_o and straightness e_s of the workpiece are negligible after the quenching and spinning, but they increase slightly after annealing due to the release of the internal stresses. The surface roughness improves greatly after spinning but becomes slightly rough after recrystallization annealing.

5 Conclusions

A new forming method to manufacture cylindrical parts with nano/ultrafine grained structures by small plastic strain is developed in this study. An experimental investigation is carried out to draw the following conclusions:

(1) A new manufacturing method consisting of quenching, power spinning and recrystallization annealing to achieve nano/ultrafine grained structures in cylindrical parts is proposed. The equivalent strain required for the power spinning is only 0.92, corresponding to a 55% thinning ratio of wall thickness.

(2) The martensite lath obtained by quenching elongates along the parallel direction of the deformation and bends along the perpendicular direction of the deformation during spinning. The lath is divided into the ultrafine regions by the dislocation wall after stagger spinning.

(3) The average thickness of the martensite laths are refined to 87 nm and a small amount of thin nanoscale deformation twins with an average thickness of 20 nm is generated after quenching and stagger spinning under 55% thinning ratio of wall thickness. The dominant mechanism of plastic deformation of the martensitic structure is dislocation slip, combined with a few of the twinning during power spinning.

(4) The equiaxed ultrafine ferrite grains with an average grain size of 160 nm are generated and the nano-carbides are precipitated in the grain boundaries after recrystallization annealing at 480°C for 30 min when the equivalent strain is only 0.92.

(5) High dimensional precision and low surface roughness of spun parts can be obtained by the proposed method.

Table 2 Calculated indexes of the macroforming quality of workpiece under different process stages

Stage	Relative wall thickness deviation Δ (%)	Ovality e_o (mm)	Straightness e_s (mm)	Roughness *R*a (μm)
Quenching	6.4	0.20	0.08	3.58
Spinning	4.5	0.20	0.11	1.27
Annealing	4.5	0.26	0.15	1.63

The relative wall thickness deviation Δ of the workpiece decreases after stagger spinning. The ovality e_o and straightness e_s of the workpiece have negligible changes after the quenching and spinning. The surface roughness decreases greatly after spinning.

(6) The spun parts with nano/ultrafine grained structures are manufactured successfully. The further study should focus on the influence of microstructure on mechanical properties of the spun parts to manufacture parts with both high strength and good ductility.

This work was supported by National Natural Science Foundation of China (Grant No. 51075153), Natural Science Foundation of Guangdong Province (Grant No. 10151040301000000), Key Laboratory of Precision Equipment and Manufacturing Technology of Guangdong Province (Grant No. PEMT1202), and the EU FP7 Marie Curie International Research Staff Exchange Scheme (IRSES) MatProFuture Project (Grant No. 318968).

1 Sauvage X, Wilde G, Divinski S V, et al. Grain boundaries in ultrafine grained materials processed by severe plastic deformation and related phenomena. Mater Sci Eng A, 2012, 540: 1–12
2 Ovid'ko I A. Deformation of nanostructures. Science, 2000, 295: 2386
3 Valiev R Z, Langdon T G. Principles of equal-channel angular pressing as a processing tool for grain refinement. Prog Mater Sci, 2006, 51: 881–981
4 Zhilyaev A P, Langdon T G. Using high-pressure torsion for metal processing: Fundamentals and applications. Prog Mater Sci, 2008, 53: 893–979
5 Guo Q, Yan H G, Chen Z H, et al. Fracture behaviors of AZ80 magnesium alloy during multiple forging process. Trans Nonferrous Met Soc China, 2006, 16: 922–926
6 Kamikawa N, Sakai T, Tsuji N. Effect of refundant shear strain on microstructure and texture evolution during accumulative roll-bonding in ultralow carbon IF steel. Acta Mater, 2007, 55: 5873–5888
7 Tsuji N, Ueji R, Minamino Y, et al. A new and simple process to obtain nano-structured bulk low-carbon steel with superior mechanical property. Scripta Mater, 2002, 46: 305–310
8 Umemoto M. Nanocrystallization of steels by severe plastic deformation. Mater Trans, 2003, 44: 1900–1911
9 Heo Y U, Suh D W, Lee H C. Fabrication of an ultrafine-grained structure by a compositional pinning technique. Acta Mater, 2014, 77: 236–247
10 Xia Q X, Xiao G F, Long H, et al. A review of process advancement of novel metal spinning. Int J Mach Tools Manuf, 2014, 85: 100–121
11 Wang L, Long H. Roller path design by tool compensation in multi-pass conventional spinning. Mater Des, 2013, 46: 645–653
12 Wang L, Long H, Ashley D, et al. Effects of roller feed ratio on wrinkling failure in conventional spinning. P I Mech Eng B-J Eng, 2011, 225: 1991–2006
13 Yang B J, Xia Q X, Cheng X Q, et al. Deformation mechanism of Nano/ultrafine grained cylindrical parts fabricated by power spinning (in Chinese). J South China Univ Tech, 2013, 41: 90–94
14 Xia Q X, Xiao G F, Long H, et al. A study of manufacturing tubes with nano/ultrafine grain structure by stagger spinning. Mater Des, 2014, 59: 516–523
15 Mishra A. Microstructural Evolution in Ultra-Fine Grained Copper Processed by Severe Plastic Deformation. San Diego: Dissertation of University of California, 2007
16 Ueji R, Tsuji N, Minamino Y, et al. Ultragrain refinement of plain low carbon steel by cold-rolling and annealing of martensite. Acta Mater, 2002, 50: 4117–4189
17 Du L X, Yao S J, Hu J, et al. Fabrication and microstructural control of nano-structured bulk steels: A review. Acta Metall Sin (Engl Lett), 2014, 27: 508–520
18 Yang B J, Xia Q X, Cheng X Q. Investigation on fabrication of ultrafine-grain tubular parts though power spinning (in Chinese). J Funct Mater, 2012, S2: 266–269
19 Deng W Y. Metallurgical Technology (In Chinese). Beijing: HigherEducation Press, 1990
20 Zeng C, Xia Q X, Xiao G F, et al. Study on cylinders spinning methods of small strain difference based on numerical simulation (in Chinese). Forg Stamp Tech, 2014, 39: 36–41
21 Xiao G F, Xia Q X, Cheng X Q, et al. Research on the grain refinement method of cylindrical parts by power spinning. Int J of Adv Manuf Tech, 2014, 78: 971–979
22 Cui Z Q, Qin Y C. Metallography and Heat Treatment (in Chinese). Beijing: China Machine Press, 2007
23 Xia Q X, Cheng X Q, Hu Y, et al. Finite element simulation and experimental investigation on the forming forces of 3D non-axisymmetrical tubes spinning. Int J Mech Sci, 2006, 48: 726–735
24 Chen G X, Jia W D, Cao G S. Process and Equipment of Power Spinning (in Chinese). Beijing: Press of National Defence Industry, 1986
25 Wang C H, Liu K Z. Spinning Technology (in Chinese). Beijing: China Machine Press, 1986
26 Xia Q X, Zhang P, Cheng X Q, et al. Orthogonal experimental study on forming process parameters of tube stagger spinning (in Chinese). Forg Stamp Tech, 2012, 37: 42–46
27 Xia Q X, Susumu S S, Kotera H. A study of the one-path drawing spinning of cups. J Mater Process Tech, 2005, 159: 397–400
28 Metal Treating Institute & China Construction Machinery Association. Heat Treatment (in Chinese). Beijing: China Machine Press, 2008
29 Kitahara H, Ueji R, Tsuji N, et al. Crystallographic features of lath martensite in low-carbon steel. Acta Mater, 2006, 54: 1279–1288
30 Wang J M, Zhou K K, Lu J. Influence of stacking fault energy on grain-refining during sever shear deformation (in Chinese). Jixie Gongcheng Xuebao, 2008, 44: 126–131
31 Lu L, Shen Y F, Chen X H, et al. Ultrahigh strength and high electrical conductivity in copper. Science, 2004, 304: 422–426
32 Xu S L, Li L F, Yuan W Y, et al. Effect of deformation on the temper process of lath martensite (in Chinese). J Univ Sci Tech Beijing, 2007, 29: 901–906
33 Hosseini S M, Najafizadeh A, Kermanpur A. Producing nano/ultrafine grained low carbon steel by martensite process using plane strain compression. J Mater Process Tech, 2011, 211: 230–236
34 Zhang T, Li M. Interchangeability and Measuring Technology (in Chinese). Beijing: Tsinghua University Press, 2010